

Model predictive control of autonomous underwater vehicles for trajectory tracking with external disturbances

Zheping Yan, Peng Gong, Wei Zhang^{*}, Wenhua Wu

College of Automation, Harbin Engineering University, 150001, China

ARTICLE INFO

Keywords:

Autonomous underwater vehicle
Fully-actuated system
Model predictive control
Trajectory tracking

ABSTRACT

This paper designs a novel double closed-loop three-dimensional (3-D) trajectory tracking method based on model predictive control (MPC) for an autonomous underwater vehicle (AUV) under external disturbances. Different from the conventional model predictive control, the designed double closed-loop control can be divided into two stages: 1) the outer-loop controller generates the desired speed instruction and passes it to the inner-loop speed controller; 2) the inner-loop speed controller generates the available control inputs to ensure the whole closed-loop trajectory tracking. In the controller design stage, the actual constraints on system inputs and state are effectively considered. In order to ensure the smooth operation of AUV, the double closed-loop controller takes the control increments as the control inputs. In addition, the stability analysis based on Lyapunov method proves the nominal stability of the controller. Finally, simulation experiments are designed to verify the tracking performance of the AUV under external disturbances. The results show the effectiveness of the controller.

1. Introduction

Autonomous underwater vehicle (AUV) is an important tool for human exploration and observation of the ocean. In the past two decades, AUV is widely used in deep-sea exploration (Zhang et al., 2015), natural hydrothermal vent observation (Sato et al., 2014) and oil spill monitoring (Choyekh et al., 2015). AUV improves the ability of human exploration while reducing the risks that human beings originally need to face. In order to ensure that the AUV can complete various special underwater tasks efficiently and accurately, it is necessary to carry out further research on the 3-D space motion control technology (Yu et al., 2019). However, AUV is a typical nonlinear, strongly coupled system. Since parameters such as hydrodynamic parameters are difficult to be accurately solved and the working environment is complex, the motion of AUV is greatly affected by the uncertainty of model parameters and external interference. The control of AUV has always been a research hotspot in the field of control.

Trajectory tracking is the basis and premise for AUV to perform various tasks. The controller is designed to drive the AUV to accurately track the time-varying trajectory from the initial state, that is, the spatial position error and velocity error converge to zero. It emphasizes the simultaneous satisfaction in the relationship between time and space,

and has strong time constraints on the task state. Up to now, scholars from all over the world have done a lot of research on the AUV trajectory tracking, and many classical control methods have been promoted. For example, Lyapunov direct method, backstepping control, model predictive control (MPC), sliding mode control, neural network and robust adaptive control, etc.

Since AUV is a multi-input and multi-output system, the Lyapunov function is constructed through iterative recursion by using backstepping control, which can simplify the design of complex control system step by step. By combining Lyapunov method with backstepping control, the velocity estimation of the vehicle is realized, and the problem of output feedback control which AUV speed feedback unfeasible is solved (Liu et al., 2009; Du et al., 2011; Xia et al., 2015). In 2014, Sun et al., (2014) proposed a filtering backstepping control method based on the biological-inspired model, which not only avoids the frequent derivation of virtual control variables, but also avoids the phenomenon of “jumping” in the vehicle’s speed response even if there is a large initial position tracking error. Unfortunately, the backstepping control itself does not have the ability to solve the uncertainty of system parameters and external disturbances, other robust adaptive technologies are integrated to ensure the effectiveness of the controller in the uncertainty of the system.

* Corresponding author.

E-mail address: dawizw@163.com (W. Zhang).

The advantage of sliding mode control is that the state of the system can reach and slide along the sliding mode surface in a finite time by switching the control variables, and it is invariant under parameter perturbation and external environment disturbance (Cheng et al., 2007). In 2015, Kim et al. (2015) proposed an anti-saturation integral sliding mode controller to solve the modeling error and unknown environmental disturbance of UUV. The equivalent control law and the switching control law are integrated to ensure the exponential stability of the trajectory tracking control system. In 2019, Qiao and Zhang (2019) designed the non-singular terminal sliding mode controller and further utilized the respective advantages of integral sliding mode and terminal sliding mode on the basis of the original controller, and proposed the double closed-loop integral terminal sliding mode control to improve the convergence and ensure the control accuracy. However, the sliding mode control method may cause a kind of undesirable high-frequency oscillation called “chattering” on the sliding mode surface, resulting in low control precision and high energy consumption (Hammad et al., 2017).

The introduction of fuzzy function and neural network can improve the adaptive learning ability of the system. Wang and Er (2016) and Hassanein et al. (2016) respectively designed direct adaptive and model-based fuzzy controllers in 2016. Sun and Ge (2014) and Zhao et al. (2014) respectively adopted neural network adaptive control in 2014 to solve the 3-DOF UUV horizontal trajectory tracking. Since then, the learning ability of neural networks has also been fully explored. For example, Dai et al. (2014, 2016) designed adaptive neural network output feedback controllers in 2014 and 2016. In 2017, Cui et al. (2017) considered the problem of control input nonlinearity and proposed neural network control with enhanced learning. However, the fuzzy logic and the performance of neural network adaptive controller depend heavily on fuzzy rules and the number of neural network nodes, resulting in a large amount of system computation, which is not conducive to the practical application of engineering.

Robust adaptive technology can modify and maintain the performance of the controller for system parameter perturbation and disturbance dynamics, and it is also widely used in AUV trajectory tracking control. In 2016, Sarhadi et al. (2016) integrated the anti-saturation compensator into the adaptive control design to solve the problem of UUV model uncertainty and propeller saturation, and proposed the model reference adaptive PID controller. In 2018, Verma et al. (2018) proposed a discrete adaptive controller to minimize the uncertainty of online parameter estimation due to the difficulty in accurately obtaining the UUV hydrodynamic coefficient in a time-varying marine environment. In addition, Zhao and Guo (2018) constructed a novel extended state observer based on non-smooth function in 2018 to estimate the system uncertainties and the state information of the vehicle. Its adaptive control performance is significantly better than the existing linear extended state observer scheme. However, in practical applications, the external disturbances suffered by AUV are usually time-varying, and the system parameters cannot be accurately obtained with the difference of motion state tasks.

Model predictive control can be optimized by predicting the future system state and output, processing real-time interference in time, ensuring the tracking performance and closed-loop system stability. In 2017, Shen et al. (2017) proposed a novel Receding Horizon Control (RHC) scheme to solve the problem of planning and tracking the planar trajectory of UUV, and gave the stability condition of UUV trajectory tracking control based on MPC for the first time. In 2018, Fan et al. (2018) proposed to use MPC to correct the vehicle's motion state and system output online in the process of autonomous underwater recovery of UUV, and combined with Kalman filter navigation guidance algorithm to estimate and compensate ocean currents in real time. In 2019, Zhang et al. (2019) proposed a model prediction controller with the speed increment as the control input, taking into account the input constraint and state constraint at the same time, and conducted simulation verification under various interferences. The author uses

kinematics as a framework to design a controller that inversely seeks control forces through velocity. On the one hand, the control force is not conducive to acting on the thrusters. On the other hand, this controller design lacks Proof of stability.

In this paper, the trajectory tracking problem of AUV is analyzed, and a novel double closed-loop controller based on MPC is designed. In order to provide robustness and adaptability, the designed double closed-loop MPC controller consisting of position loop and speed loop ensures accurate tracking of time-varying trajectories. To ensure the smooth operation of the AUV, the control increment is taken as the input of the inner-loop and the outer-loop. The actual constraints of system input and state are fully considered in the design of the controller, and the trajectory tracking problem is transformed into a standard quadratic programming problem with constraints that can be calculated online. When the AUV moves to a new position, the optimal input for the next moment is recalculated according to the current state and expectations. Therefore, the AUV can still complete the target tracking task well under the complex ocean environments. To prove the effectiveness of the controller, the tracking simulation results are given. The simulation results prove the effectiveness of the designed controller.

The rest of this paper is organized as follows: Section 2 gives the mathematical model for fully-actuated AUV. Section 3 presents the control block diagram of double closed-loop MPC and designs the MPC controller in detail. Section 4 demonstrates the stability of the controller. Simulation results and conclusions are given in Section 5 and 6, respectively.

2. AUV model

2.1. Kinematic model

To study the motion model of underwater robot, the motion of underwater robot is approximated to the general motion of rigid body in fluid. According to the origin of the coordinate system, the coordinate system is divided into fixed coordinate system $E - \xi\eta\zeta$ and motion coordinate system $O - xyz$. The former is defined as a fixed point on the earth, while the latter is defined as AUV. The coordinate system satisfies the right-hand Cartesian rectangular coordinate system. The positive direction is north, east and down, as shown in Fig. 1.

The fixed coordinate system $E - \xi\eta\zeta$ describes the AUV's spatial position and attitude. $\eta = [\xi \eta \zeta \phi \theta \psi]$ is defined in a fixed coordinate system, where heading angle ψ , trim angle θ , heel angle ϕ all represent the angle of AUV motion coordinate system relative to fixed coordinate

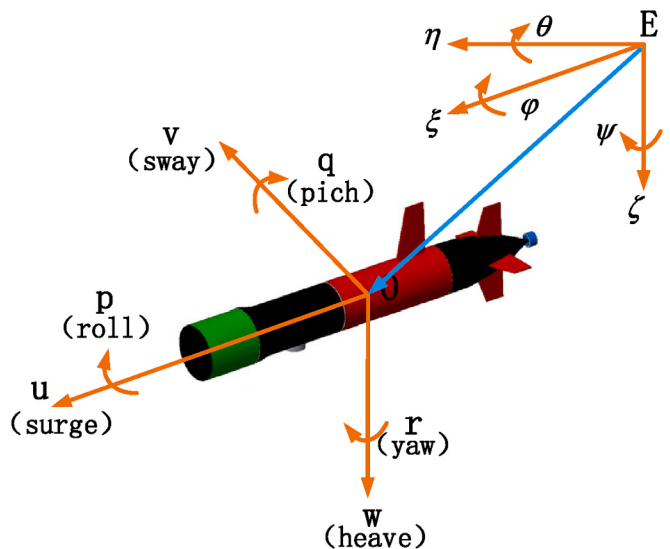


Fig. 1. AUV coordinate system.

system. $\nu = [u \ v \ w \ p \ q \ r]$ is defined in a motion coordinate system, where u, v, w are the longitudinal, transverse vertical, speeds respectively. p, q, r respectively represent the roll angle speed, pitch angle speed and heading angular speed. To avoid the singular problem of Euler Angle, the trim angle θ is bounded which satisfying $-\pi/2 < \theta < \pi/2$. In practice, the trim angle θ cannot approach $\pi/2$ due to metacentric restoring force (Do and Pan, 2009). In general, the roll motion is regarded as self-stable and the roll amplitude is very small, which can be regarded as the heel angle $\phi = 0$ and heel angular velocity $p = 0$.

The relationship between η and ν are expressed by the following formula:

$$\dot{\eta} = J(\eta)\nu \quad (1)$$

where

$$J(\eta) = \begin{bmatrix} J_1(\eta) & \theta_{3*2} \\ \theta_{2*3} & J_2(\eta) \end{bmatrix} \quad (2)$$

$$J_1(\eta) = \begin{bmatrix} \cos \psi \cos \theta & -\sin \psi & \sin \theta \cos \psi \\ \sin \psi \cos \theta \cos \psi & \sin \psi \sin \theta & -\sin \theta \\ 0 & 0 & \cos \theta \end{bmatrix} \quad (3)$$

$$J_2(\eta) = \begin{bmatrix} 1 & 0 \\ 0 & 1/\cos \theta \end{bmatrix} \quad (4)$$

$J(\eta)$ is transition matrix, θ_{3*2} is a 3×2 zero matrix, θ_{2*3} is a 2×3 zero matrix, $J_1(\eta)$ is linear velocity transformation matrix, $J_2(\eta)$ is angular velocity transformation matrix. θ and ψ are Euler Angle in Fig. 1.

2.2. Dynamic model

According to the AUV model proposed by Fossen, its vector representation is

$$M\dot{\nu} + C(\nu)\nu + D(\nu) + g(\eta) = \tau \quad (5)$$

M is inertial matrix, $M = M_{RB} + M_A$. M_{RB} is rigid body mass matrix, $M_{RB} = \text{diag}(m, m, m, I_y, I_z)$. M_A is additional inertia matrix, $M_A = \text{diag}(-X_{\dot{u}}, -Y_{\dot{v}}, -Z_{\dot{w}}, -M_{\dot{q}}, -N_r)$. m is the mass of AUV, I_y and I_z are inertial tensors, $X_{\dot{u}}$, $Y_{\dot{v}}$, $Z_{\dot{w}}$, $M_{\dot{q}}$ and N_r are measurable hydrodynamic coefficients.

$C(\nu)$ is Coriolis and centripetal matrix, $C(\nu) = C_{RB}(\nu) + C_A(\nu)$. $C_{RB}(\nu)$ is rigid body Coriolis force and centripetal force matrix, $C_A(\nu)$ is hydrodynamic Coriolis force and centripetal force matrix.

where

$$C_{RB} = \begin{bmatrix} 0 & 0 & 0 & mw & -mv \\ 0 & 0 & 0 & 0 & mu \\ 0 & 0 & 0 & -mu & 0 \\ -mw & 0 & mu & 0 & 0 \\ mv & -mu & 0 & 0 & 0 \end{bmatrix} \quad (6)$$

$$C_A = \begin{bmatrix} 0 & 0 & 0 & -Z_{\dot{w}}w & Y_{\dot{v}}v \\ 0 & 0 & 0 & 0 & -X_{\dot{u}}u \\ 0 & 0 & 0 & X_{\dot{u}}u & 0 \\ Z_{\dot{w}}w & 0 & -X_{\dot{u}}u & 0 & 0 \\ -Y_{\dot{v}}v & X_{\dot{u}}u & 0 & 0 & 0 \end{bmatrix} \quad (7)$$

$D(\nu)$ is hydrodynamic damping matrix, which indicates the viscous force of the fluid on the AUV. $D(\nu) = \text{diag}\{X_u, Y_v, Z_w, M_q, N_r\} + \text{diag}\{X_{|u|u}|u|, Y_{|v|v}|v|, Z_{|w|w}|w|, M_{|q|q}|q|, N_{|r|r}|r|\}$, where $X_u, Y_v, Z_w, M_q, N_r, X_{|u|u}|u|, Y_{|v|v}|v|, Z_{|w|w}|w|, M_{|q|q}|q|$ and $N_{|r|r}|r|$ are measurable hydrodynamic coefficients.

$g(\eta)$ represents the vector of restoring forces and moments due to gravity and buoyancy. Since the center of gravity and center of buoyancy must be designed on the Z axis, and the AUV is generally assumed to have zero buoyancy. So, $W = mg$, $B = \rho gV$, $W = Bx_g = x_b y_g = y_b$,

$$g(\eta) = [0 \ 0 \ 0 \ \rho gV\overline{GM_L} \sin \theta \ 0]^T. W$$
 is the gravity, B is the

buoyancy, $\overline{GM_L}$ is the vertical metacentric height. $\tau = [\tau_u \ \tau_v \ \tau_w \ \tau_q \ \tau_r]^T$ is the input forces and moments for each degree of freedom.

3. Design of double closed loop MPC controller

This paper focuses on AUV 3-D trajectory tracking in complex ocean environments. The main control objective is to ensure that all dynamic characteristics of AUV keep consistent with position and speed with the change of time. The whole closed-loop system control design includes inner and outer loops. The outer loop position control uses the system output feedback to design the expected speed, so as to ensure the convergence of AUV position tracking error. The inner loop speed control uses the system actual control input to realize that the driving speed of the AUV gradually converges to the desired speed command, that is to ensure the convergence of AUV speed tracking error. Considering the corresponding constraints when designing each controller could find the optimal solution in the control set more efficiently. The control design block diagram of the whole closed-loop system is shown in Fig. 2.

3.1. MPC-based outer-loop controller

It is assumed that the 3-D trajectory is given in advance and is smooth and bounded. The desired trajectory can be described as follows:

$$Y_d = [\xi_d \ \eta_d \ \zeta_d \ \theta_d \ \psi_d]^T \quad (8)$$

In this section, the control task is to design the desired speed to drive the AUV by inputting position error. The kinematic model is discretized with a sampling period T_s . The discrete model is obtained as follows:

$$\eta(k+1) = \eta(k) + J(k)\nu(k)T_s \quad (9)$$

In order to make the speed change of AUV stable, the velocity increment is taken as the control input. The improved state space model can be reformulated as:

$$x_\eta(k+1) = A_{d\eta}(k)x_\eta(k) + B_{d\eta}(k)\Delta u_\nu(k) \quad (10)$$

$$y_\eta(k) = C_{d\eta}(k)x_\eta(k) \quad (11)$$

with

$$x_\eta(k) = [\eta(k) \ \nu(k-1)]^T \quad (12)$$

$$\Delta u_\nu(k) = \nu(k) - \nu(k-1) \quad (13)$$

$$A_{d\eta}(k) = \begin{bmatrix} I_5 & J(k)T_s \\ 0_5 & I_5 \end{bmatrix} \quad (14)$$

$$B_{d\eta}(k) = \begin{bmatrix} J(k)T_s \\ I_5 \end{bmatrix} \quad (15)$$

$$C_{d\eta} = [I_5 \ 0_5] \quad (16)$$

where I_5 is a 5×5 identity matrix, 0_5 is a 5×5 zero matrix.

The future dynamics of the system can be deduced based on the model. Assuming that all the states are measurable. Set N_{p1} as prediction horizon, N_{c1} as control horizon, $N_{c1} \leq N_{p1}$.

Defining Y_η as N_{p1} step predicted output vector, ΔU_ν as N_{c1} step input vector:

$$Y_\eta = \begin{bmatrix} y_\eta(k+1|k) \\ y_\eta(k+2|k) \\ \vdots \\ y_\eta(k+N_{p1}|k) \end{bmatrix} \quad (17)$$

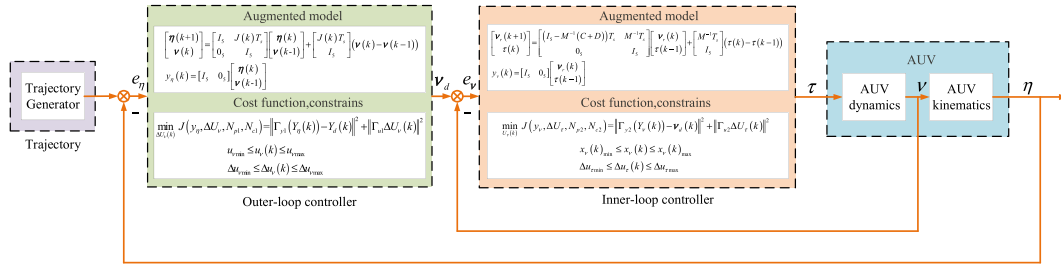


Fig. 2. Diagram of the AUV control framework.

$$\Delta U_\nu = \begin{bmatrix} \Delta u_\nu(k) \\ \Delta u_\nu(k+1) \\ \vdots \\ \Delta u_\nu(k+N_{c1}-1) \end{bmatrix} \quad (18)$$

Based on the model predictive control principle, the predictive equation expression can be derived as follows:

$$Y_\eta = S_{x1}x_\eta(k) + S_{u1}\Delta U_\eta \quad (19)$$

where

$$S_{x1} = \begin{bmatrix} C_{d\eta}A_{d\eta} & C_{d\eta}A_{d\eta}^2 & \cdots & C_{d\eta}A_{d\eta}^{N_{p1}} \end{bmatrix}^T \quad (20)$$

$$S_{u1} = \begin{bmatrix} C_{d\eta}B_{d\eta} & 0 & \cdots & 0 \\ C_{d\eta}A_{d\eta}B_{d\eta} & C_{d\eta}B_{d\eta} & \cdots & 0 \\ \vdots & \vdots & \ddots & \vdots \\ C_{d\eta}A_{d\eta}^{N_{p1}-1}B_{d\eta} & C_{d\eta}A_{d\eta}^{N_{p1}-2}B_{d\eta} & \cdots & C_{d\eta}A_{d\eta}^{N_{p1}-N_{c1}}B_{d\eta} \end{bmatrix} \quad (21)$$

There are some constraints when AUV performs trajectory tracking tasks. When designing the outer-loop position controller, the amplitude of the control input \$u_\nu(k)\$ and control input increment \$\Delta u_\nu(k)\$ will be considered as constraints. The amplitude of the control input \$u_\nu(k)\$ has an upper bound and a lower bound, and control input increment \$\Delta u_\nu(k)\$ is also limited.

$$u_{\nu\min} \leq u_\nu(k) \leq u_{\nu\max} \quad (22)$$

$$\Delta u_{\nu\min} \leq \Delta u_\nu(k) \leq \Delta u_{\nu\max} \quad (23)$$

where \$u_{\nu\min}, \Delta u_{\nu\min}\$ are predefined lower bounds, \$u_{\nu\max}, \Delta u_{\nu\max}\$ are predefined upper bounds.

The amplitude of the control input \$u_\nu(k)\$ constraints are converted into control input increment \$\Delta u_\nu(k)\$ constraints and expressed as the following compact linear constraint forms:

$$M_1\Delta U_\nu \leq \gamma_1 \quad (24)$$

where

$$\begin{aligned} M_1 &= \begin{bmatrix} I \\ -I \\ C_2 - C_1 \end{bmatrix}, \gamma_1 = \begin{bmatrix} \Delta U_{\nu\max} - \Delta U_{\nu\min} \\ u_{\nu\max} - C_1 u(k-1) - u_{\nu\min} + C_1 u(k-1) \end{bmatrix}, C_1 \\ &= \begin{bmatrix} I_5 \\ I_5 \\ \vdots \\ I_5 \end{bmatrix}, C_2 = \begin{bmatrix} I_5 & 0 & \cdots & 0 \\ I_5 & I_5 & \cdots & 0 \\ \vdots & \vdots & \ddots & \vdots \\ I_5 & I_5 & \cdots & I_5 \end{bmatrix} \end{aligned} \quad (25)$$

Select the following objective function:

$$\min_{\Delta U_\nu(k)} J(Y_\eta, \Delta U_\nu, N_{p1}, N_{c1}) = \| \Gamma_{y1}(Y_\eta(k)) - Y_d(k) \|^2 + \| \Gamma_{u1}\Delta U_\nu(k) \|^2 \quad (26)$$

where \$\Gamma_{y1}\$ and \$\Gamma_{u1}\$ denote the weighting factor of output signal and the weighting factors of control signal, respectively.

The quadratic equation about \$\Delta U_\nu\$ can be obtained by taking \$Y_\eta\$ into

the objective function. The final standard convex quadratic programming form can be written as follows:

$$\begin{aligned} \Delta U_\nu^*(k) &= \underset{\Delta U_\nu(k)}{\operatorname{argmin}} \left(\frac{1}{2} \Delta U_\nu^T(k) H_1(k) \Delta U_\nu(k) + f_1^T(k) \Delta U_\nu(k) \right) \\ &\text{s.t.} \quad M_1 \Delta U_\nu \leq \gamma_1 \end{aligned} \quad (27)$$

where

$$H_1(k) = - \left(S_{u1}^T \Gamma_{y1}^T \Gamma_{y1} S_{u1} + \Gamma_{u1}^T \Gamma_{u1} \right) \quad (28)$$

$$f_1(k) = \left(S_{u1}^T \Gamma_{y1}^T \Gamma_{y1} (S_{x1}x_\eta(k) - Y_d(k)) \right) \quad (29)$$

The transformed quadratic programming problem can be calculated online. Then, the optimal input vector \$\Delta U_\nu^*(k)\$ for the prediction can be obtained. But only the first element of \$\Delta U_\nu^*(k)\$ is the input.

$$\Delta u_\nu(k) = \Delta U_\nu^*(k|k) \quad (30)$$

According to the following formula, \$\nu(k)\$ can be obtained and used as the expected speed of the inner-loop controller.

$$\nu_d(k) = \nu(k) = \nu(k-1) + \Delta \nu(k) = \nu(k-1) + \Delta u_\nu^*(k) \quad (31)$$

3.2. MPC-based inner-loop controller

The control task in this section is to design the force and moment driving the AUV based on the input velocity error. The dynamic model is discretized and the sampling period is \$T_s\$. Since the values of restoring forces and moments are relatively small, they are ignored in order to facilitate the design of the controller. The discrete model is obtained as follows:

$$\nu_r(k+1) = (I - M^{-1}(C + D)) T_s \nu_r(k) + M^{-1} T_s \tau \quad (32)$$

where \$\nu_r = \nu - \nu_{ed}\$, \$\nu_{ed}\$ is the ocean current velocity \$\nu_c\$ or random disturbance velocity \$\nu_{rd}\$.

To make the force and moment change of AUV stable, the force and moment increment are taken as the control input. The improved state space model can be reformulated as:

$$x_v(k+1) = A_{dv}(k)x_v(k) + B_{dv}(k)\Delta u_\tau(k) \quad (33)$$

$$y_v(k) = C_{dv}(k)x_v(k) \quad (34)$$

with

$$x_v(k) = [\nu_r(k) \quad \tau(k-1)]^T \quad (35)$$

$$\Delta u_\tau(k) = \tau(k) - \tau(k-1) \quad (36)$$

$$A_{dv}(k) = \begin{bmatrix} (I_5 - M^{-1}(C + D)) T_s & M^{-1} T_s \\ 0_5 & I_5 \end{bmatrix} \quad (37)$$

$$B_{dv}(k) = \begin{bmatrix} M^{-1} T_s \\ I_5 \end{bmatrix} \quad (38)$$

$$C_{dv} = [I_5 \quad 0_5] \quad (39)$$

where I_5 is a 5×5 identity matrix, 0_5 is a 5×5 zero matrix.

Assuming that all the states are measurable. Set N_{p2} as prediction horizon, N_{c2} as control horizon, $N_{c2} \leq N_{p2}$. Defining Y_ν as N_{p2} step predicted output vector, ΔU_τ as N_{c2} step input vector:

$$Y_\nu = \begin{bmatrix} y_\nu(k+1|k) \\ y_\nu(k+2|k) \\ \vdots \\ y_\nu(k+N_p|k) \end{bmatrix} \quad (40)$$

$$\Delta U_\tau = \begin{bmatrix} \Delta u_\tau(k) \\ \Delta u_\tau(k+1) \\ \vdots \\ \Delta u_\tau(k+N_c - 1) \end{bmatrix} \quad (41)$$

Based on the model predictive control principle, the predictive equation expression can be derived as follows:

$$Y_\nu = S_{x2}x_\nu(k) + S_{u2}\Delta U_\tau \quad (42)$$

where

$$S_{x2} = \begin{bmatrix} C_{dv}A_{dv} & C_{dv}A_{dv}^2 & \cdots & C_{dv}A_{dv}^{N_{p2}} \end{bmatrix}^T \quad (43)$$

$$S_{u2} = \begin{bmatrix} C_{dv}B_{dv} & 0 & \cdots & 0 \\ C_{dv}A_{dv}B_{dv} & C_{dv}B_{dv} & \cdots & 0 \\ \vdots & \vdots & \ddots & \vdots \\ C_{dv}A_{dv}^{N_{p2}-1}B_{dv} & C_{dv}A_{dv}^{N_{p2}-2}B_{dv} & \cdots & C_{dv}A_{dv}^{N_{p2}-N_{c2}}B_{dv} \end{bmatrix} \quad (44)$$

When designing the inner-loop position controller, the state of the system $x_\nu(k)$ and control input increment $\Delta u_\tau(k)$ will be considered as constraints. The state of the system $x_\nu(k)$ has an upper bound and a lower bound, and control input increment $\Delta u_\tau(k)$ is also limited.

$$x_\nu(k)_{\min} \leq x_\nu(k) \leq x_\nu(k)_{\max} \quad (45)$$

$$\Delta u_{\tau\min} \leq \Delta u_\tau(k) \leq \Delta u_{\tau\max} \quad (46)$$

where $x_\nu(k)_{\min}$, $\Delta u_{\tau\min}$ are predefined lower bounds, $x_\nu(k)_{\max}$, $\Delta u_{\tau\max}$ are predefined upper bounds.

The state of the system $x_\nu(k)$ constraints are converted into control input increment $\Delta u_\tau(k)$ constraints and expressed as the following compact linear constraint forms:

$$M_2\Delta U_\tau \leq \gamma_2 \quad (47)$$

where

$$M_2 = \begin{bmatrix} I_5 - I_5 \\ B_{dv}(k) - B_{dv}(k) \end{bmatrix}, \gamma_2 = \begin{bmatrix} \Delta U_{\tau\max} - \Delta U_{\tau\min} \\ X_{\nu\max} - A_{dv}(k) - X_{\nu\min} + A_{dv}(k) \end{bmatrix} \quad (48)$$

Select the following objective function:

$$\min_{U_\tau(k)} J(y_\nu, \Delta U_\tau, N_{p2}, N_{c2}) = \| \Gamma_{y2}(Y_\nu(k)) - \nu_d(k) \|^2 + \| \Gamma_{u2}\Delta U_\tau(k) \|^2 \quad (49)$$

where Γ_{y2} and Γ_{u2} denote the weighting factor of output signal and the weighting factors of control signal, respectively.

The quadratic equation about $\Delta U_\tau(k)$ can be obtained by taking Y_ν into the objective function. The final standard convex quadratic programming form can be written as follows:

$$\Delta U_\tau^*(k) = \underset{\Delta U_\tau(k)}{\operatorname{argmin}} \left(\frac{1}{2} \Delta U_\tau^T(k) H_2(k) \Delta U_\tau(k) + f_2^T(k) \Delta U_\tau(k) \right) \quad (50)$$

$$\text{s.t. } M_2\Delta U_\tau \leq \gamma_2$$

where

$$H_2(k) = - \left(S_{u2}^T \Gamma_{y2}^T \Gamma_{y2} S_{u2} + \Gamma_{u2}^T \Gamma_{u2} \right) \quad (51)$$

$$f_2(k) = \left(S_{u2}^T \Gamma_{y2}^T (S_{x2}x_\nu(k) - \nu_d(k)) \right) \quad (52)$$

The transformed quadratic programming problem can be calculated online. Then, the optimal input vector $\Delta U_\tau^*(k)$ for the prediction can be obtained. But only the first element of $\Delta U_\tau^*(k)$ is the input.

$$\Delta u_\tau(k) = \Delta U_\tau^*(k|k) \quad (53)$$

According to the following formula, $\tau(k)$ can be obtained and applied to AUV.

$$\tau^*(k) = \tau(k-1) + \Delta \tau(k) = \tau(k-1) + \Delta u_\tau^*(k) \quad (54)$$

The $\Delta u_\tau^*(k)$ is calculated at each sampling time k . The AUV repeatedly computes and performs optimal control forces and moments $\tau^*(k)$ to achieve receding horizon optimization. The predicted state $x_\nu(k+1)$ and the optimal input $\Delta u_\tau^*(k)$ are determined by the current state $x_\nu(k)$. Thus, the MPC could compensate for the system uncertainties caused by model mismatch and external disturbances (Zhang et al., 2019). The rolling optimization process is iterated until the AUV trajectory tracking task is completed. It can be seen that MPC can reduce the impact of model uncertainty. This article focuses on practical engineering applications and therefore focuses on the impact of external perturbations on AUV trajectory tracking.

4. Stability analysis

In this section, the stability of the MPC-based double closed-loop controller is demonstrated as follows.

Theorem 1. For the MPC-based outer-loop controller (9), consider the cost function (26) with the constraints (24). Select positive definite matrix Γ_{y1} , positive definite matrix Γ_{u1} , predictive horizon N_{p1} , control horizon N_{c1} and guarantee the optimal solution of the cost function (26) exists. Select the optimal cost function $J^*(k)$ as a Lyapunov function $V^*(k)$. If $V^*(k+1) \leq V^*(k)$ satisfies, then the optimal solution $\Delta U_\nu^*(k)$ guarantees nominal stable of the system (9).

Proof: In the optimal solution $\Delta U_\nu^*(k)$ of the cost function (26) with constraints (24), select $\Delta u_\nu^*(k+i|k)$ be the optimal control input increment. Then $u_\nu^*(k+i|k)$ is the optimal control input corresponding to the optimal control input increment $\Delta u_\nu^*(k+i|k)$. The optimal cost function $J^*(k)$ is selected as a Lyapunov function $V^*(k)$.

$$\begin{aligned} V^*(k) &= \min J(k) \\ &= \min \left[\sum_{i=1}^{N_{p1}} \| \Gamma_{y1}(y_\eta(k+i|k)) - y_d(k+i|k) \|^2 + \sum_{i=0}^{N_{c1}-1} \| \Gamma_{u1}\Delta u_\nu(k+i|k) \|^2 \right] \end{aligned} \quad (55)$$

Clearly, the optimal function (55) satisfies $V^*(0)=0$ with $k=0$ and $V^*(k)>0$ with arbitrary $k \neq 0$. For system (9) with external disturbances, the optimal control input increments $\Delta u_\nu(k+1+i|k+1)$ and control input $u_\nu(k+1+i|k+1)$ are shown as follows:

$$\begin{aligned} \Delta u_\nu(k+1+i|k+1) &= [\Delta u_\nu(k+1|k+1), \Delta u_\nu(k+2|k+1), \dots, \Delta u_\nu(k+N_{c1}|k+1)] \\ &= [\Delta u_\nu^*(k+1|k+1), \Delta u_\nu^*(k+2|k+1), \dots, \Delta u_\nu^*(k+N_{c1}|k+1)] \end{aligned} \quad (56)$$

$$\begin{aligned} u_\nu(k+1+i|k+1) &= [u_\nu(k+1|k+1), u_\nu(k+2|k+1), \dots, u_\nu(k+N_{c1}|k+1)] \\ &= [u_\nu^*(k+1|k+1), u_\nu^*(k+2|k+1), \dots, u_\nu^*(k+N_{c1}|k+1)] \end{aligned} \quad (57)$$

It is straightforward to Proof that (56), (57) are feasible solutions for the quadratic programming (27). The control increment $\Delta u_\nu(k+1+i|k+1)$ and the controller $u_\nu(k+1+i|k+1)$ are satisfy the constraint sets (22) and (23), respectively. According to (56), (57), the

relation between $V^*(k)$ and $J(k+1)$ are displayed as follows:

$$V^*(k+1) \leq J(k+1) \leq V^*(k) - \|\Gamma_{y1}(y_\eta^*(k)) - y_d(k)\|^2 - \|\Gamma_{u1}\Delta u_\nu^*(k)\|^2 \quad (58)$$

where

$$\begin{aligned} J(k+1) &= \sum_{i=1}^{N_{p1}} \|\Gamma_{y1}(y_\eta(k+1+i|k+1)) - y_d(k+1+i|k+1)\|^2 + \sum_{i=0}^{N_{c1}} \|\Gamma_{u1}\Delta u_\nu(k+1+i|k+1)\|^2 \\ &= \sum_{i=2}^{N_{p1}} \|\Gamma_{y1}(y_\eta^*(k+i|k)) - y_d(k+i|k)\|^2 + \sum_{i=1}^{N_{c1}-1} \|\Gamma_{u1}\Delta u_\nu^*(k+i|k)\|^2 \\ &= \sum_{i=1}^{N_{p1}} \|\Gamma_{y1}(y_\eta^*(k+i|k)) - y_d(k+i|k)\|^2 + \sum_{i=0}^{N_{c1}-1} \|\Gamma_{u1}\Delta u_\nu^*(k+i|k)\|^2 \\ &\quad - \|\Gamma_{y1}(y_\eta(k|k)) - y_d(k|k)\|^2 - \|\Gamma_{u1}\Delta u_\nu(k|k)\|^2 \\ &= V^*(k) - \|\Gamma_{y1}(y_\eta(k|k)) - y_d(k|k)\|^2 - \|\Gamma_{u1}\Delta u_\nu(k|k)\|^2 \end{aligned} \quad (59)$$

In addition, function $J(k+1)$ is not less than $V^*(k+1)$ due to optimality of the cost function (27).

$$V^*(k+1) \leq V^*(k) \quad (60)$$

The Lyapunov function (55) satisfies $V^*(0) = 0$ for $k = 0$ and $V^*(k) > 0$ for arbitrary $k \neq 0$. The Lyapunov function (55) is monotonically decreasing i.e. $V^*(k+1) \leq V^*(k)$. Thus, system (9) is nominally stable.

For the MPC-based inner-loop controller (32), [Theorem 1](#) is equally applicable. So, the relevant proofs are not made.

5. Simulation results

In this section, the simulation results prove the effectiveness and robustness of the proposed double closed-loop MPC controller.

Parameters related to AUV studied by [Pettersen and Egeland \(1999\)](#) are given in [Table 1](#). The relevant parameter values of the double closed loop MPC controller are as follows: sampling period $T_s = 0.5$ s, prediction horizon $N_{p1} = N_{p2} = 40$, control horizon $N_{c1} = N_{c2} = 4$, weighted factor $\Gamma_{y1} = \Gamma_{y2} = \text{diag}(0.01, 0.01, 0.01, 0.01, 0.01, 0.01)$, $\Gamma_{u1} = \Gamma_{u2} = \text{diag}(1, 1, 1, 1, 1)$, the amplitude of the control input constraints $u_{\max} = [2, 1, 1, 0.05, 0.05]^T$, $u_{\min} = [-2, -1, -1, -0.05, -0.05]^T$, input constraints $\Delta u_{\max} = [0.2, 0.15, 0.15, 0.05, 0.05]^T$, $\Delta u_{\min} = [-0.2, -0.15, -0.15, -0.05, -0.05]^T$, $\Delta u_{\min} = [-50, -50, -50, -10, -10]^T$, $\Delta u_{\max} = [50, 50, 50, 10, 10]^T$, state constraints $x_\nu(k)_{\max} = [2, 1.5, 1.5, \pi/18, \pi/18, 200, 200, 200, 50, 50]^T$, $x_\nu(k)_{\min} =$

Table 1
Values of the AUV parameters.

Parameters	Value	Parameters	Value
m	185 kg	Y_ν	100 kg/s
X_u	-30 kg	$Y_{ \nu }$	200 kg/m
$Y_\dot{\nu}$	-80 kg	Z_w	100 kg/s
$Z_{\dot{w}}$	-80 kg	$Z_{ \dot{w} }$	200 kg/m
I_y	40 kgm ²	M_q	50 kgm ² /s-rad
M_q	-40 kgm ²	$M_{ q }$	100 kgm ² /rad ²
I_z	40 kgm ²	N_r	50 kgm ² /(s-rad)
N_r	-40 kgm ²	$N_{ r }$	100 kgm ² /rad ²
X_u	70 kg/s	$X_{ u }$	100 kg/m

$$[-2, -1.5, -1.5, -\pi/18, -\pi/18, -200, -200, -200, -50, -50]^T.$$

There are three kinds of disturbances in the marine environment: ocean wave disturbance, ocean current disturbance and random disturbance. Because this paper focuses on trajectory tracking in deep ocean environment, ocean wave disturbance is not considered. Both types of disturbances are defined in fixed coordinate system $E - \xi\eta\zeta$. The

ocean current disturbance is defined as follows:

$$\begin{cases} u_c = 0.15 \text{ m/s} \\ v_c = 0.15 \text{ m/s} \end{cases} \quad (61)$$

The random disturbance is defined as follows:

$$\begin{cases} u_{rd} = 0.2 \times \text{rand}(1) \text{ m/s} \\ v_{rd} = 0.2 \times \text{rand}(1) \text{ m/s} \end{cases} \quad (62)$$

where $\text{rand}(1)$ is a normal distribution noise signal with 0 mean and 1 variance.

The desired trajectory of the simulation is a spiral diving trajectory as shown in (62). The initial state of AUV is $[0, 5, 0, 0, 0]^T$.

$$\begin{cases} x_d = 10 \sin(0.03t) \\ y_d = 10 \cos(0.03t) \\ z_d = -0.05t \end{cases} \quad (63)$$

[Fig. 3](#) shows the trajectories tracking results of the three methods without disturbance in 3-d space. The black curve is the desired trajectory, the red curve is the tracking result using designed MPC method, the light blue curve is the tracking result using conventional MPC method, and the purple curve shows the tracking result using terminal

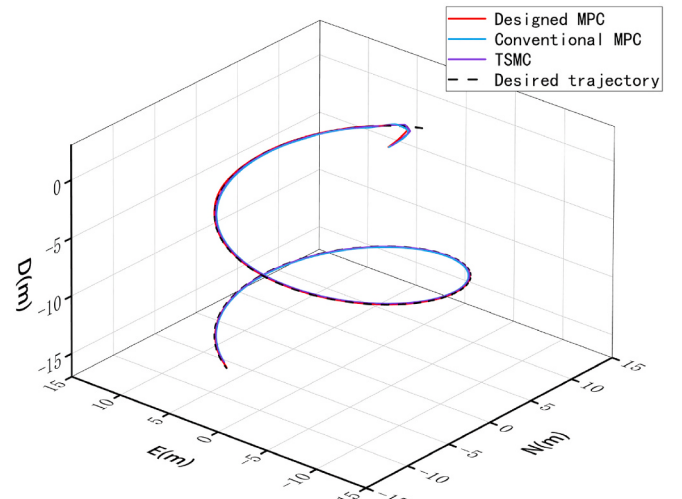


Fig. 3. AUV 3-D trajectories for spiral tracking without disturbance.

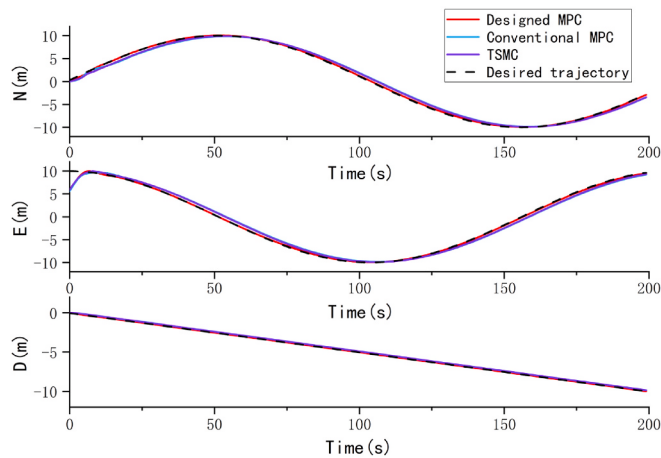


Fig. 4. Position tracking performances for tracking task without disturbance.

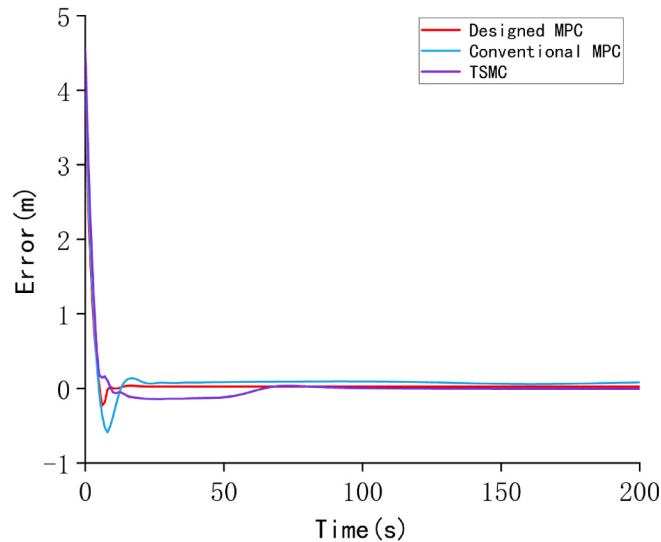


Fig. 5. Position tracking errors for tracking task without disturbance.

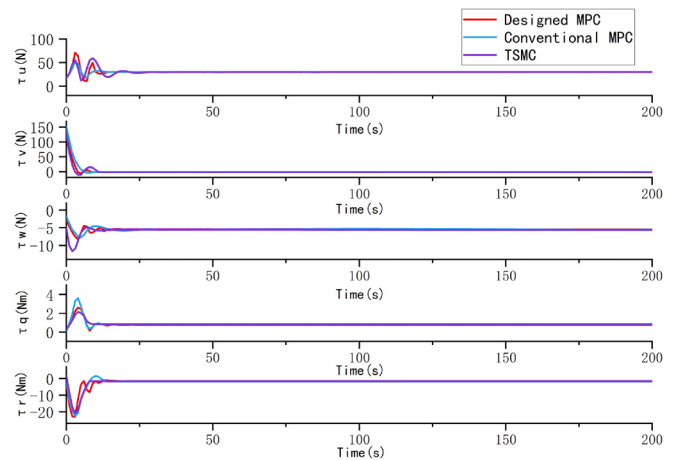


Fig. 6. Control inputs of the AUV without disturbance.

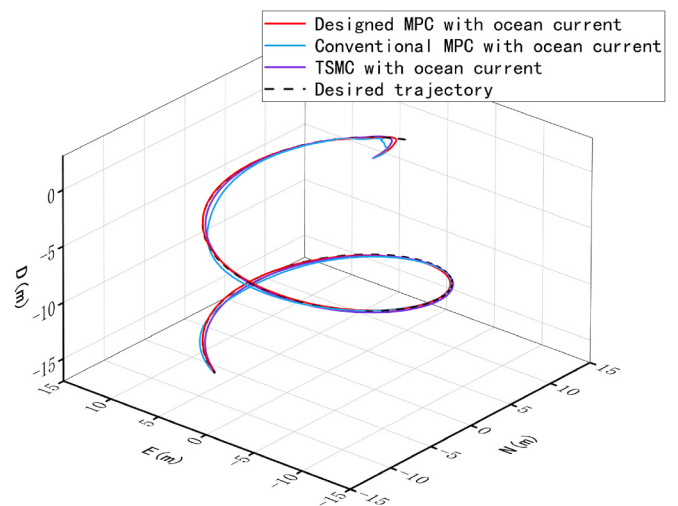


Fig. 7. AUV 3-D trajectories for spiral tracking with ocean current.

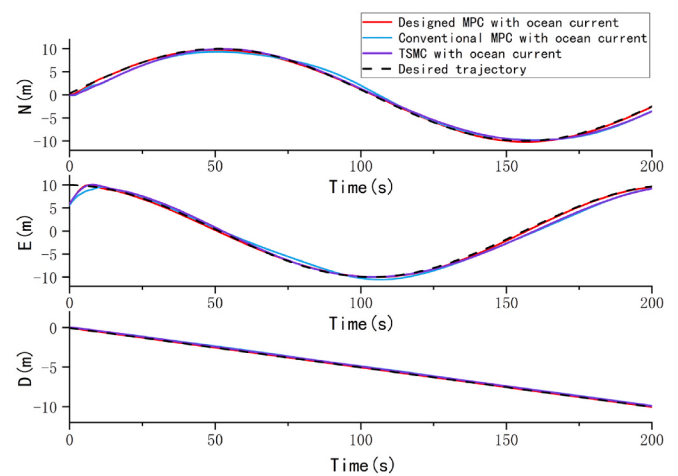


Fig. 8. Position tracking performances for tracking task with ocean current.

Table 2
Position error measurement values after 20 s without disturbance.

Methods	Maximum(m)	Minimum(m)	Average(m)
Designed MPC	0.0253	0.0133	0.0253
Conventional MPC	0.0943	0.0697	0.0783
TSMC	0.0361	0.0151	0.0271

sliding mode control (TSMC). It can be seen from the figure that all three methods are well tracked on the desired trajectory.

The tracking performance in the three directions and position tracking error of AUV are shown in Fig. 4 and Fig. 5, respectively. In general, the AUV tracking control has a better tracking effect under different control methods. Position tracking errors are bounded. For further comparison, the position error measurement values after 20 s are indicated in Table 2. It can be seen from the table that the designed MPC method without disturbance has the best tracking results compared to the other two methods. The value of the position tracking error of the AUV without disturbance is very small (about 0.0253 m). The control inputs of the AUV are shown in Fig. 6. The control inputs without disturbance are stable and change slowly.

The trajectories tracking results of the three methods with ocean current in 3-d space are displayed in Fig. 7. Fig. 8 and Fig. 9 are the

tracking performance in the three directions and position tracking error of AUV, respectively. It can be seen from the figure that the designed MPC method is superior to the other two methods. Position tracking errors are also bounded. For clarity of comparison, the position error

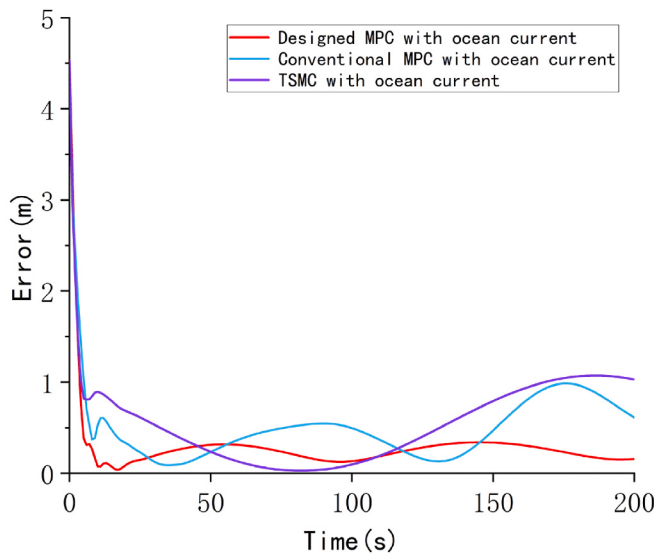


Fig. 9. Position tracking errors for tracking task with ocean current.

Table 3

Position error measurement values after 20 s with ocean current.

Methods	Maximum(m)	Minimum(m)	Average(m)
Designed MPC	0.3353	0.1255	0.2201
Conventional MPC	0.9855	0.0897	0.3258
TSMC	1.0724	0.0292	0.3519

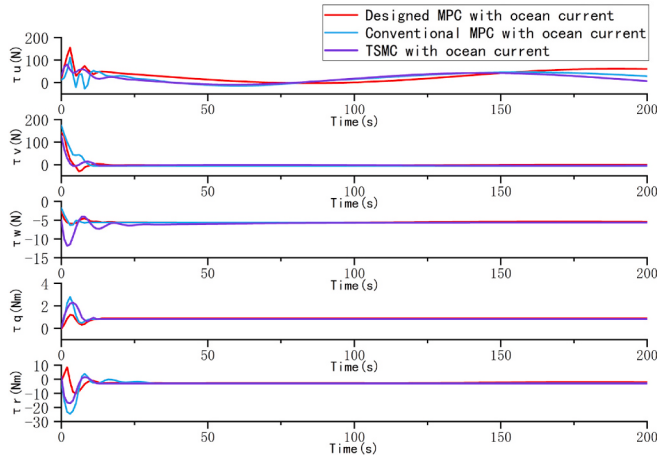


Fig. 10. Control inputs of the AUV with ocean current.

measurement values after 20 s are displayed in **Table 3**. The value of the position tracking error of the AUV without disturbance is about 0.2201 m. **Fig. 10** shows the control inputs of the AUV.

The trajectories tracking results of the three methods with random disturbance are displayed in **Fig. 11**. The tracking performance in the three directions and position tracking error of AUV are shown in **Fig. 12** and **Fig. 13**, respectively. Position tracking errors are bounded. For further comparison, the position error measurement values after 20 s are indicated in **Table 4**. It can be seen from the table that the designed MPC method with random disturbance has a better tracking effect compared to the other two methods. The value of the position tracking error of the AUV without disturbance is very small (about 0.1398m). The control inputs of the AUV are displayed in **Fig. 14**. The simulation results with random disturbance further demonstrate the robustness of the designed MPC method.

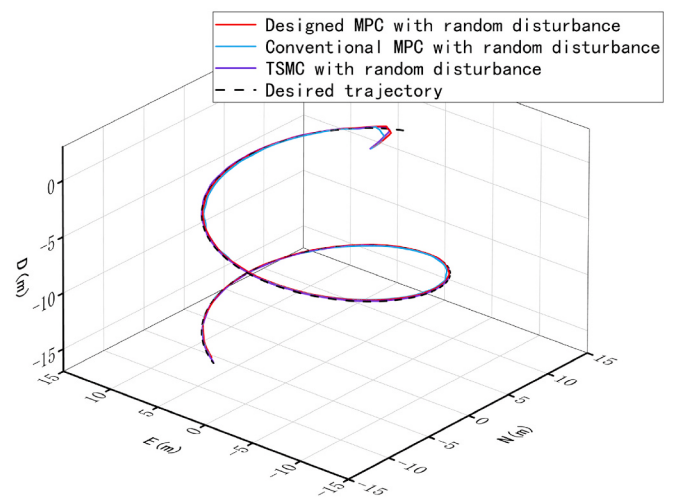


Fig. 11. AUV 3-D trajectories for spiral tracking with random disturbance.

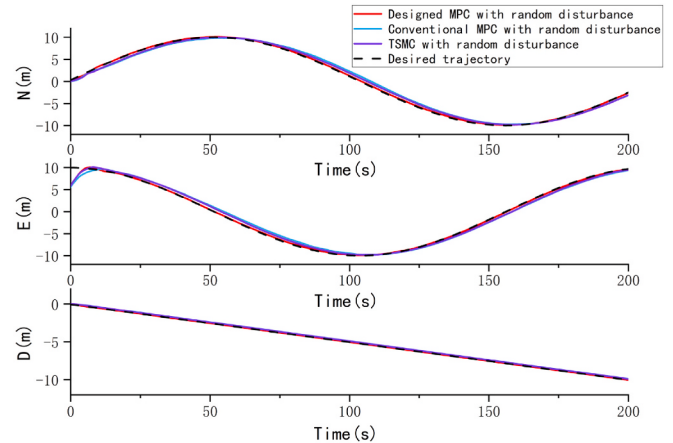


Fig. 12. Position tracking performances for tracking task with random disturbance.

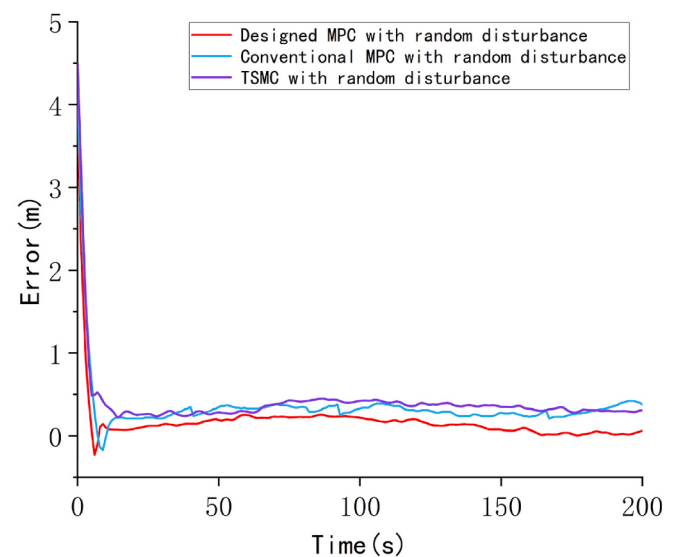


Fig. 13. Position tracking errors for tracking task with random disturbance.

Table 4

Position error measurement values after 20 s with random disturbance.

Methods	Maximum(m)	Minimum(m)	Average(m)
Designed MPC	0.2454	0.0183	0.1398
Conventional MPC	0.3910	0.2112	0.3019
TSMC	0.4501	0.2330	0.3423

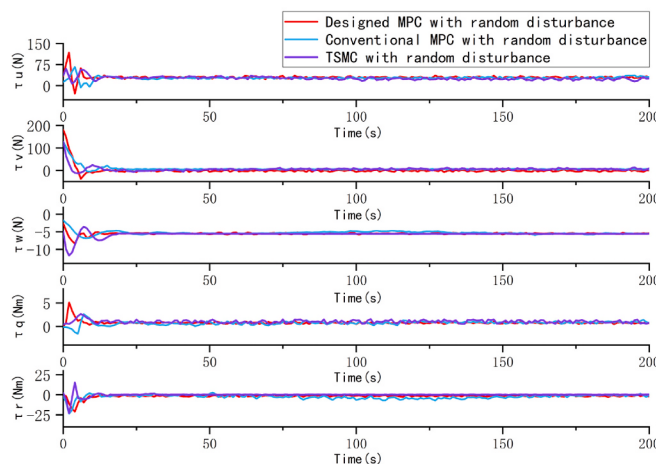


Fig. 14. Control inputs of the AUV with random disturbance.

6. Conclusion

This paper designs a double closed-loop trajectory tracking method for AUV based on model predictive control. Firstly, the 5-DOF model of a fully-actuated AUV is established according to kinematics and dynamics methods. Then, the AUV outer-loop position controller and inner-loop speed controller are designed respectively. The outer-loop controller generates the desired speed instruction and passes it to the inner-loop speed controller, while the inner-loop speed controller generates the available control inputs to ensure the whole closed-loop trajectory tracking. Next, the outer-loop controller introduces velocity increment as input, and the inner-loop controller introduces forces and moments increment as input. At the same time, the constraints of system input and state are explicitly considered, which improves the stable operation capability of AUV. The receding horizon implementation enables the optimal control inputs to be recalculated at each sampling moment, which can compensate for the system uncertainty caused by model mismatch and external disturbance. Finally, simulation experiments are designed and the results show the effectiveness of the controller.

In our follow-up research, we not only consider the impact of external disturbances, but also consider other issues in many aspects. And that includes the uncertainty of model parameters under AUV high-speed motion, the output feedback control problem of AUV under the condition of unmeasurable speed state information, limited bandwidth for underwater acoustic communication and time delays in communication systems and so on.

CRediT authorship contribution statement

Zheping Yan: Conceptualization, Funding acquisition, Writing - review & editing. **Peng Gong:** Methodology, Simulation, Writing - original draft. **Wei Zhang:** Writing - review & editing, Supervision, Project administration. **Wenhua Wu:** Visualization, Investigation.

Declaration of competing interest

The authors declare that they have no known competing financial interests or personal relationships that could have appeared to influence the work reported in this paper.

Acknowledgements

This work was supported by National Natural Science Foundation of China (the funding number is No.51679057), National Natural Science Foundation of China under Grant No.51609046 and the Province Science Fund for Distinguished Young Scholars No. J2016JQ0052, Ph.D. Student Research and Innovation Fund of the Fundamental Research Funds for the Central Universities (the funding number is No.3072020GIP0410).

References

- Cheng, J., Yi, J., Zhao, D., 2007. Design of a sliding mode controller for trajectory tracking problem of marine vessels. *IET Control Theory & Appl.* 1 (1), 233–237.
- Choyekh, M., Kato, N., Short, T., et al., 2015. Vertical water column survey in the Gulf of Mexico using autonomous underwater vehicle SOTAB-I. *Mar. Technol. Soc. J.* 49 (3), 88–101.
- Cui, R., Yang, C., Li, Y., et al., 2017. Adaptive neural network control of AUVs with control input nonlinearities using reinforcement learning. *IEEE Trans. Syst. Man Cybern.: Systems* 47 (6), 1019–1029.
- Dai, S.L., Wang, M., Wang, C., 2016. Neural learning control of marine surface vessels with guaranteed transient tracking performance. *IEEE Trans. Ind. Electron.* 63 (3), 1717–1727.
- Dai, S.L., Wang, M., Wang, C., et al., 2014. Learning from adaptive neural network output feedback control of uncertain ocean surface ship dynamics. *Int. J. Adapt. Contr. Signal Process.* 28, 341–365.
- Do, K.D., Pan, J., 2009. *Control of Ships and Underwater Vehicles: Design for Underactuated and Nonlinear Marine Systems*. Springer-Verlag, London, U.K.
- Du, J., Yu, S., Zhao, Y., et al., 2011. Semi-global output feedback tracking control for fully actuated ships. *Asian J. Contr.* 13 (4), 570–575.
- Fan, S., Li, B., Xu, W., et al., 2018. Impact of current disturbances on AUV docking: model-based motion prediction and countering approach. *IEEE J. Ocean. Eng.* 43 (4), 888–904.
- Hammad, M.M., Elshenawy, A.K., El Singaby, M.I., 2017. Trajectory following and stabilization control of fully actuated AUV using inverse kinematics and self-tuning fuzzy PID. *PLoS One* 12 (7), e0179611.
- Hassanein, O., Anavatti, S.G., Shim, H., et al., 2016. Model-based adaptive control system for autonomous underwater vehicles. *Ocean Eng.* 127, 58–69.
- Kim, M., Joe, H., Kim, J., et al., 2015. Integral sliding mode controller for precise maneuvering of autonomous underwater vehicle in the presence of unknown environmental disturbances. *Int. J. Contr.* 88 (10), 2055–2065.
- Liu, S., Wang, D., Poh, E., 2009. Output feedback control design for station keeping of AUVs under shallow water wave disturbances. *Int. J. Robust Nonlinear Control* 19, 1447–1470.
- Pettersen, K.Y., Egeland, O., 1999. Time-varying exponential stabilization of the position and attitude of an underactuated autonomous underwater vehicle. *IEEE Trans. Automat. Contr.* 44 (1), 112–115.
- Qiao, L., Zhang, W.D., 2019. Double-loop integral terminal sliding mode tracking control for UUVs with adaptive dynamic compensation of uncertainties and disturbances. *IEEE J. Ocean. Eng.* 44 (1), 29–53.
- Sarhadi, P., Noei, A.R., Khosravi, A., 2016. Model reference adaptive PID control with anti-windup compensator for an autonomous underwater vehicle. *Robot. Autonom. Syst.* 83, 87–93.
- Sato, Y., Maki, T., Kume, A., et al., 2014. Path replanning method for an AUV in natural hydrothermal vent fields: toward 3D imaging of a hydrothermal chimney. *Mar. Technol. Soc. J.* 48 (3), 104–114.
- Shen, C., Shi, Y., Buckham, B., 2017. Integrated path planning and tracking control of an AUV: a unified receding horizon optimization approach. *IEEE ASME Trans. Mechatron.* 22 (3), 1163–1173.
- Sun, B., Zhu, D., Yang, S.X., 2014. A bioinspired filtered backstepping tracking control of 7000-m manned submarine vehicle. *IEEE Trans. Ind. Electron.* 61 (7), 3682–3693.
- Sun, X., Ge, S.S., 2014. Adaptive neural region tracking control of multi-fully actuated ocean surface vessels. *IEEE/CAA J. Automat. Sin.* 1 (1), 77–83.
- Verma, S., Shen, D., Xu, J.X., 2018. Motion control of robotic fish under dynamic environmental conditions using adaptive control approach. *IEEE J. Ocean. Eng.* 43 (2), 381–390.

- Wang, N., Er, M.J., 2016. Direct adaptive fuzzy tracking control of marine vehicles with fully unknown parametric dynamics and uncertainties. *IEEE Trans. Contr. Syst. Technol.* 24 (5), 1845–1852.
- Xia, G.Q., Shao, X.C., Zhao, A., 2015. Robust nonlinear observer and observer-backstepping control design for surface ships. *Asian J. Contr.* 17 (4), 1377–1393.
- Yu, H., Guo, C., Yan, Z., 2019. Globally finite-time stable three-dimensional trajectory-tracking control of underactuated UUVs. *Ocean Eng.* 109, 106329.
- Zhang, Y., Liu, X., Luo, X., et al., 2019. MPC-based 3-D trajectory tracking for an autonomous underwater vehicle with constraints in complex ocean environments. *Ocean Eng.* 189.
- Zhang, F., Marani, G., Smith, R.N., Choi, H.T., 2015. Future trends in marine robotics. *IEEE Robot. Autom. Mag.* 22 (1), 14–122.
- Zhao, Z., He, W., Ge, S.S., 2014. Adaptive neural network control of a fully actuated marine surface vessel with multiple output constraints. *IEEE Trans. Contr. Syst. Technol.* 22 (4), 1536–1543.
- Zhao, Z.L., Guo, B.Z., 2018. A novel extended state observer for output tracking of MIMO systems with mismatched uncertainty. *IEEE Trans. Automat. Contr.* 63 (1), 211–218.